Geochemical Perspectives Letters

Young oxygenation of the Archean Keonjhar Palaeosol, India, from ^{138}La-^{138}Ce chronometry

M.L. Pfennig[1*], J.J. Pakulla[1], E. Hasenstab-Dübeler[1], F. Wombacher[1], J. Jodder[2,3,4], A. Hofmann[4,5], C. Münker[1]

https://doi.org/10.7185/geochemlet.2503

Abstract

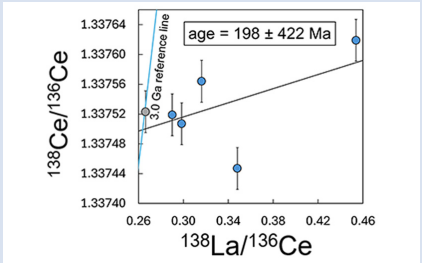

Though there is increasing evidence from different geochemical proxies for intermittent oxygenation prior to the Great Oxidation Event (GOE), it remains ambiguous whether post-depositional processes altered these proxy signals. In this regard, the *ca*. 3.0 Ga old Keonjhar Palaeosol in the Singhbhum Craton in India has received particular attention, as the presence of Ce anomalies in this Archean palaeosol has been interpreted to reflect oxic surface weathering conditions during the Mesoarchean. Trace element analyses from this study revealed only small or no Ce anomalies and depleted REE patterns relative to the protolith. Most importantly, ^{138}La-^{138}Ce chronometry constrains a ^{138}La-^{138}Ce age of <620 Ma. This result precludes previous claims for Archean atmospheric oxygenation preserved in the Keonjhar palaeosol. Corresponding ^{147}Sm-^{143}Nd data yielded an isochron age of 1765 ± 180 Ma and ^{176}Lu-^{176}Hf data do not define an isochron. Altogether, these results indicate post-Archean REE mobilisation. Our findings emphasise the importance of combining palaeo-redox-proxies with radiogenic isotope analysis to validate their significance.

Received 7 March 2024 | Accepted 5 January 2025 | Published 7 February 2025

Introduction

The evolution of complex life on Earth is closely linked to the presence of free oxygen in the atmosphere. The Great Oxidation Event (GOE) describes the first rise in free oxygen from >10^{-5} PAL to >10^{-2} PAL (Present Atmospheric Level), starting at *ca*. 2.45 Ga (*e.g.*, Farquhar *et al.*, 2007). The source of oxygen is generally ascribed to oxygenic photosynthesis, which led to the development of local oxygen oases in the marine realm well before the GOE (*e.g.*, Planavsky *et al.*, 2014). The reconstruction of oxygen levels in Earth's atmosphere and hydrosphere through deep time is typically based on various palaeo-redox proxies in terrestrial and marine sedimentary rocks and palaeosols (*e.g.*, Rye and Holland, 1998; Lyons *et al.*, 2014; Catling and Zahnle, 2020). In this regard, the anomalous behaviour of Ce relative to other REE provides a key palaeo-redox proxy, as Ce can be oxidised to highly insoluble Ce^{4+} (*e.g.*, Tostevin, 2021). Accordingly, water–rock interaction under oxidising conditions leads to a decoupling of Ce^{4+} from the remaining REE^{3+}. Soil horizons may show such a decoupling, with upper oxic zones showing positive Ce anomalies due to immobility of Ce^{4+}, whereas lower, reduced soil horizons may inherit negative anomalies due to mineral authigenesis from REE^{3+}-enriched groundwaters (*e.g.*, Banfield and Eggleton, 1989). Therefore, Ce anomalies in palaeosols can yield information of ancient atmospheric O_2 levels.

One of the oldest preserved palaeosols is the *ca*. 3.0 Ga old Keonjhar Palaeosol from the Singhbhum Craton, India (Bandopadhyay *et al.*, 2010; Das *et al.*, 2012; Dzombak and Sheldon, 2022), for which Mukhopadhyay *et al.* (2014) reported the presence of negative Ce anomalies. These authors interpreted the anomalies to have formed in the Archean, at the time of pedogenesis and, therefore, serving as evidence for pre-GOE atmospheric oxygenation. However, care needs to be taken by applying palaeo-redox proxies to rocks that have potentially experienced multiple episodes of alteration, including prolonged recent surface exposure (*e.g.*, Bonnand *et al.*, 2020). Direct dating of REE^{3+}-Ce^{4+} decoupling is therefore needed. However, the application of the ^{138}La-^{138}Ce chronometer (Tanaka and Masuda, 1982) has been challenging so far, and there are only few pilot studies available (*e.g.*, Hayashi *et al.*, 2004; Bonnand *et al.*, 2020). To better understand whether Ce anomalies in the Keonjhar Palaeosol indeed record Archean weathering, we applied ^{138}La-^{138}Ce chronometry to directly date the formation of the Ce anomalies. Ion exchange chromatography and measurements of La and Ce using MC-ICP-MS were performed following the protocol of Schnabel *et al.* (2017) (see methods in the Supplementary Information for more details). To complement

1. Institute of Geology and Mineralogy, University of Cologne, Germany
2. Centre for Planetary Habitability (PHAB), University of Oslo, Norway
3. Evolutionary Studies Institute, University of the Witwatersrand, South Africa
4. Department of Geology, University of Johannesburg, South Africa
5. School of Earth, Ocean, and Climate Sciences, IIT, Bhubaneswar, India

* Corresponding author (email: pfennig.melisande@gmail.com)

the information from ^{138}La-^{138}Ce and better infer alteration conditions in general, we also analysed major and trace elements as well as ^{176}Lu-^{176}Hf and ^{147}Sm-^{143}Nd isotope compositions for samples from the Keonjhar Palaeosol. Further information on methodology is provided in the Supplementary Information.

The Keonjhar Palaeosol—Geological Background

The Keonjhar Palaeosol formed on top of the Keonjhar Bhaunra Granite (Tait *et al.*, 2011), a porphyritic feldspar-biotite granite which is part of the Singhbhum Granitoid Complex (SGC), one of the main crustal units of the Singhbhum Craton (*e.g.*, Hofmann *et al.*, 2022). The palaeosol formation age is constrained by the crystallisation of the granite at *ca*. 3.29 Ga (Tait *et al.*, 2011) and the deposition age of the overlying quartzites at *ca*. 3.02 Ga (Mukhopadhyay *et al.*, 2014). As the latter is a maximum depositional age based on detrital zircons, the age of pedogenesis is poorly constrained but clearly Archean. The overlying, cross-bedded quartzites form the base of the Koira Group, which unconformably overlies the SGC (Hofmann *et al.*, 2022). These shallow-marine quartzites represent clastic sediments that formed during craton-wide transgression of the Singhbhum Craton, associated with crustal extension (*e.g.*, Hofmann *et al.*, 2022). The sampled palaeosol outcrop lies within an operating quarry site that is located *ca*. 8 km northwest of Keonjhar (Fig. S-1). We analysed one sample representing the granitic protolith (F) and five samples (A–E) of the palaeosol profile at the palaeosurface (0 m), and at 2 m, 4 m, 5 m, and 7 m below the palaeosurface. More details are provided in the Supplementary Information, including coordinates and field photographs of outcrop locations in Figures S-1 and S-2, and photographs of hand specimens A–F in Figure S-3. The up to 10 m thick alteration zone is predominantly composed of quartz and pyrophyllite and subordinate muscovite, illite, orthoclase, plagioclase, chloritoid and tourmaline (Das *et al.*, 2012; Mukhopadhyay *et al.*, 2014; Hofmann *et al.*, 2022). Alkaline elements are strongly depleted relative to Al and Ti, as well as compared to their concentrations in the protolith (Figs. 1, S-4; Bandopadhyay *et al.*, 2010; Mukhopadhyay *et al.*, 2014). In addition to the predominance of pyrophyllite, the occurrence of increasingly abundant quartz veins towards the palaeo-surface suggests hydrothermal alteration, which could have proceeded along the unconformity plane separating the former palaeosol-surface and the overlying quartzites. The presence of a foliation and evidence for shearing indicate late-stage deformation of the palaeosol (Hofmann *et al.*, 2022).

Results and Discussion

Detailed information on major and trace element concentrations, isotope data and measurement protocols are provided in the Supplementary Information. Major and trace element patterns of the soil profile are shown in Figures 1, 2, and S-4, S-5, S-6, S-7 and S-12. Because Al is regarded as a highly immobile element, we normalised elemental abundances to Al and the element/Al to the corresponding element/Al of the protolith in Figures 1, 2, S-4, S-6 and S-7. Figure S-12 also shows selected element data without any protolith-normalisation. In Figure S-6, we show normalised data for all samples and additional data from Tait *et al.* (2011) for the Keonjhar Bhaunra Granite, which is compositionally very similar to our sample of the palaeosol protolith. However, we note strong compositional heterogeneity of palaeosol samples likely linked to heterogeneously distributed REE-rich accessory phases and small-scale REE redistribution within the alteration zone, which is discussed in more detail in the Supplementary Information, including additional trace element data (Figs. S-7 to S-11). Isochrons and age reference lines for the three isotope systems ^{138}La-^{138}Ce, ^{147}Sm-^{143}Nd and ^{176}Lu-^{176}Hf are shown in Figure 3. Lanthanum anomalies and Ce anomalies were calculated using a geometric extrapolation after Barrat *et al.* (2023) (Fig. 1i, Tables S-2, S-3) and are displayed in a PAAS-normalised plot in Figure S-5 (Pourmand *et al.*, 2012). The dataset from Mukhopadhyay *et al.* (2014) shows remarkably strong negative Ce anomalies from Ce/Ce*$_{CI}$ of 0.76 up to 0.20, while our samples show somewhat smaller Ce/Ce*$_{CI}$ of 0.82 up to 1.21 (Fig. S-5). Minor LREE mobility of the protolith is also displayed by its composition (La/La*$_{CI}$ = 0.87–0.89,

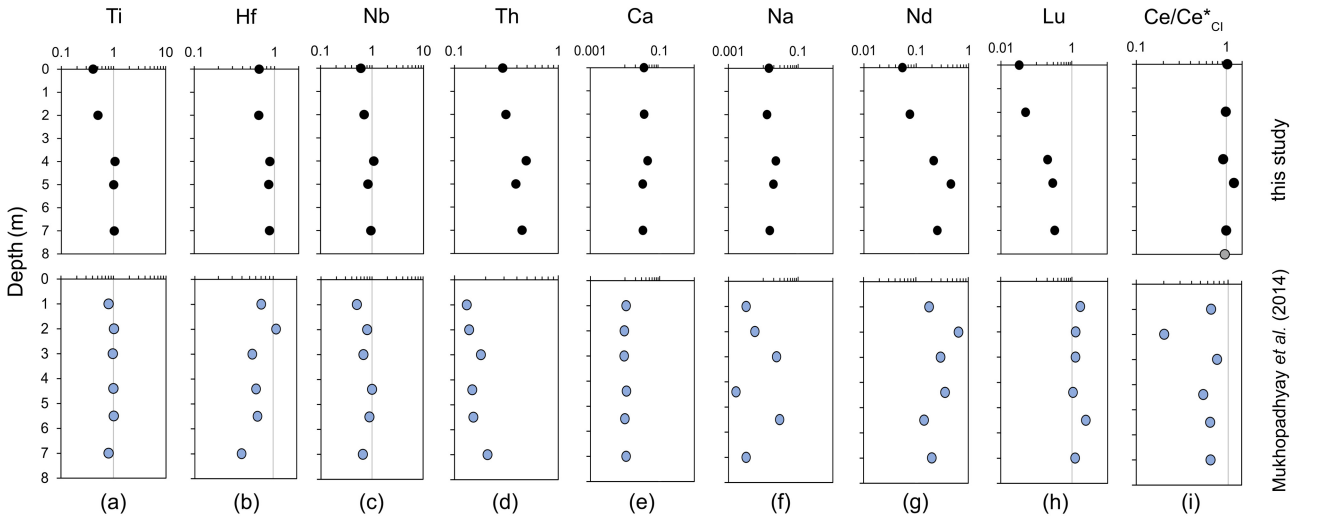

Figure 1 **(a–h)** Selected major and trace element ratios normalised to Al and the element/Al ratios are normalised to the corresponding element/Al of the granite protolith sample SIN17F (Tables S-1 and S-2). **(i)** Ce/Ce*$_{CI}$ values calculated after Barrat *et al.* (2023) (Table S-2). **(Top panels)** Palaeosol samples SIN17A-E from this study (digestion no. 4). **(Lower panels)** Data from Mukhopadhyay *et al.* (2014). The grey line represents the element ratio in the protolith sample SIN17F, which by definition is 1. Mukhopadhyay *et al.* (2014) did not provide sufficient information on outcrop location and palaeosol stratigraphy, but we assume that the authors collected the palaeosol samples from the same outcrop albeit from a different section (see text and Fig. S-1).

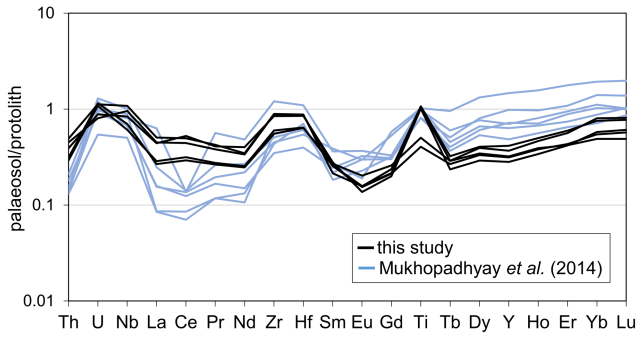

Figure 2 Protolith-normalised incompatible element data for the Keonjhar palaeosol samples from this study (digestion no. 4) and data from Mukhopadhyay *et al.* (2014). Mukhopadhyay *et al.* (2014) did not provide sufficient information on outcrop location and palaeosol stratigraphy, but we assume that their samples were collected from the same outcrop albeit from a different section (see text and Fig. S-1). Both datasets are normalised to Al and the element/Al ratios are normalised to the corresponding element/Al of the granite protolith sample SIN17F (Tables S-1 and S-2). Both datasets show LREE depletion of the palaeosol relative to the protolith and La-Ce fractionation, which likely occurred during post-Archean alteration as indicated by the isotope data (Fig. 3). The two datasets display somewhat distinct element patterns in terms of REE mobility and magnitude of Ce anomalies, which is most likely due to alteration at different fluid conditions or simply less fluid alteration.

$Ce/Ce^*_{CI} = 0.81–0.97$) (Tables S-2, S-3), which may indicate that some alteration also affected the protolith in addition to the Keonjhar Palaeosol.

The depletion of fluid-mobile elements such as alkaline earth metals (Figs. 1, 2 and S-4) implies that they were largely removed from the palaeosol. Immobile elements such as Nb, Hf and Ti show no evidence of a significant depletion relative to Al and the protolith (Figs. 1a–c, 2, S-4). These results are in good agreement with the element mobilisation patterns in the palaeosol profile studied by Mukhopadhyay *et al.* (2014) (see also Figs. 1, 2 and S-4), whereby the authors interpreted these patterns to reflect palaeo-weathering. Notably, the data from Mukhopadhyay *et al.* (2014) and our study display somewhat distinct geochemical signatures in terms of HREE mobilisation and magnitude of Ce anomalies (Figs. 1i, S-5, Tables S-2, S-3). These differences can potentially be explained by a locally different environmental setting and different fluid conditions within the alteration zone as discussed below. Unfortunately, Mukhopadhyay *et al.* (2014) did not provide detailed information on outcrop location, and we assume that their samples reflect a different profile from the same outcrop (Fig. S-1). Therefore, we limit our discussion below to possibly similar alteration processes that affected the two palaeosol profiles, rather than putting them in a direct stratigraphic context. The dissolution of REE (and Th)-rich accessory mineral phases during alteration, such as apatite, monazite, xenotime or allanite, as indicated by Th depletion in both datasets (Fig. 2), could explain the (L)REE depletion relative to the protolith in both palaeosol profiles (*e.g.*, Banfield and Eggleton, 1989; Braun *et al.*, 1993). To create negative Ce anomalies, first alteration under oxidising conditions must have occurred nearby, whereby most of the Ce^{4+} was retained and other REE^{3+} may have been complexed and removed to variable extents. Thereby, positive Ce anomalies, as for example displayed by our sample SIN17D1, were similarly generated (Figs. 1i, S-5, Tables S-2, S-3). The Ce-depleted and REE-enriched fluids might have migrated to different portions of the palaeosol at different redox or pH conditions, thereby generating slightly enriched REE patterns as observed for the palaeosol profile from Mukhopadhyay *et al.* (2014), and negative Ce anomalies as observed for both datasets (Figs. 1i, S-5, Tables S-2, S-3). Notably, our sampled portion of the palaeosol shows a lower magnitude of negative Ce anomalies and no HREE enrichment compared to the sampled section from Mukhopadhyay *et al.* (2014), which is probably due to alteration at different fluid conditions or simply less fluid alteration. Based on experimental studies, selective REE mobility occurs during hydrothermal alteration, depending on prevailing pH-values and available ligands (*e.g.*, Yongliang and Yusheng, 1991; Haas *et al.*, 1995). Therefore, considering the prevalence of pyrophyllite, and the abundance of quartz veins in the alteration zone (*e.g.*, Hofmann *et al.*, 2022), hydrothermal alteration likely played an important role in the alteration history of the Keonjhar Palaeosol rather than weathering-related processes. Either way, Ce oxidation requires the involvement of oxic fluids at least at some point in the alteration history.

Our ^{138}La-^{138}Ce dating approach (Fig. 3a) yields an errorchron age of 198 ± 422 Ma. The expected ^{138}Ce ingrowth for an Archean La-Ce fractionation event is illustrated by the 3 Ga reference line in Figure 3a, which is clearly not supported by our dataset. Rather, our samples show a narrow range in present-day $^{138}Ce/^{136}Ce$ ratios but a large spread in La/Ce ratios (from 0.2663 to 0.4538), indicating only small ingrowth of ^{138}Ce and, therefore, likely a more recent and post-depositional fractionation of La from Ce. Even though this result neither rules out the possibility of previously formed Ce anomalies nor the influence of recent weathering, it demonstrates unambiguously that the Ce anomalies in the Keonjhar Palaeosol cannot be taken as direct evidence for an elevated Mesoarchean oxygen partial pressure, as suggested by Mukhopadhyay *et al.* (2014). Rather, our finding agrees with observations arguing for post-depositional overprint of the Keonjhar Palaeosol (Hofmann *et al.*, 2022). Furthermore, this result aligns with evidence from Hayashi *et al.* (2004) and Bonnand *et al.* (2020), also applying ^{138}La-^{138}Ce chronometry to date purported Archean Ce anomalies. In both studies of ~3.2 Ga old sedimentary rocks from the Barberton Greenstone Belt, South Africa, Ce mobility was found to be linked to much later post-depositional alteration.

In addition to ^{138}La-^{138}Ce dating, ^{176}Lu-^{176}Hf isotope data (Fig. 3c) yield no isochron, which also argues for REE mobilisation. As outlined in Figure 2, the ^{176}Lu-^{176}Hf data reflect depletion of the HREE relative to Zr-Hf. The large deviation of our ^{176}Lu-^{176}Hf data from the 3 Ga reference line suggests that it does not reflect Archean Lu-Hf fractionation. If we take the calculated ages at face value and assume both La-Ce and Lu-Hf were fractionated by the same process, the REE mobility could be recent to as old as Neoproterozoic in age, which is in agreement with late Mesozoic and Cenozoic alteration patterns previously reported for BIFs from the Koira Group higher up in the stratigraphy (Beukes *et al.*, 2008). However, the modern-day $^{176}Hf/^{177}Hf$ values are unradiogenic and almost indistinguishable, only differing within 20 % from one another, and this might suggest that Lu and Hf were barely mobilised and fractionated since protolith emplacement. This is also supported by the constant Hf/Al ratios in our sampled palaeosol profile, showing hardly any evidence for element mobilisation (Fig. 1b). Compared to the other REE, Lu also shows the smallest depletion relative to the protolith (Figs. 1h and 2). The immobility of Hf and Lu could be related to residual mineral phases in the palaeosol, which are more resistant to alteration, as for example Lu and Hf bearing zircon.

In addition to the clearly post-Archean alteration of ^{138}La-^{138}Ce, the ^{147}Sm-^{143}Nd system yields an isochron age of 1765 ± 180 Ma (Fig. 3b) and therefore indicates Proterozoic

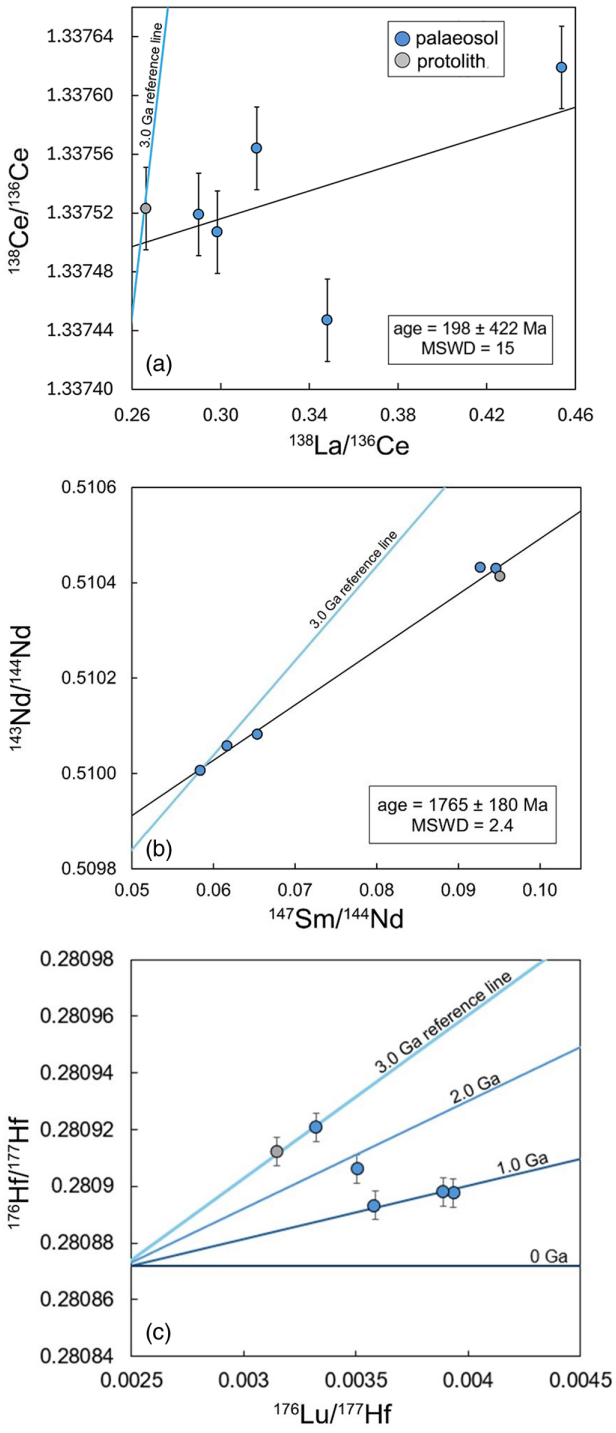

Figure 3 Radiogenic isotope compositions of palaeosol samples SIN17A to E (blue) and protolith sample SIN17F (grey). Errorchrons and age reference lines were calculated using MS Excel and Isoplot 2.49 for MS Excel (Ludwig, 2001). Error bars show external reproducibility. See Supplementary Information for further information on calculations and isotope measurements. Plots shown are **(a)** ^{138}La-^{138}Ce, **(b)** ^{147}Sm-^{143}Nd and, for **(c)** ^{176}Lu-^{176}Hf, only age reference lines are shown. Error bars are smaller than symbol sizes for ^{147}Sm-^{143}Nd.

LREE mobility. This is in line with the elemental depletion of LREE relative to the protolith, displayed in both palaeosol datasets (Figs. 1, 2). Also, it implies that Sm-Nd and Lu-Hf (considering the similar Lu/Hf ratios to the protolith) were less fractionated by younger alteration events than La-Ce, as suggested by ^{138}La-^{138}Ce dating. This difference can be explained by selective LREE complexation during hydrothermal alteration events as discussed above (*e.g.*, Yongliang and Yusheng, 1991). Potentially, this is because of the immobile character of Ce^{4+} among the REE, which probably triggers a more pronounced fractionation of La-Ce than of Sm-Nd and Lu-Hf during alteration events.

Altogether, our data indicate a complex alteration history for the Keonjhar Palaeosol, including multiple element mobilisation events and depletion of mobile major and trace elements, and REE in the palaeosol profile. This depletion is reflected in datasets from this study and Mukhopadhyay *et al.* (2014), and illustrated in Figures 1, 2 and S-4. Element depletion is likely due to fluid flow along the unconformity plane separating the former palaeosol-surface and the overlying quartzites at various times in the long geological history of the succession. Clear field evidence (Hofmann *et al.*, 2022), suggesting hydrothermal overprint and later deformation of the palaeosol, in combination with geochemical evidence (Fig. 3), indicate alteration events that cannot reflect Mesoarchean palaeo-weathering conditions. Rather, our combined ^{147}Sm-^{143}Nd and ^{138}La-^{138}Ce data argue for multiple, post-Archean alteration events of the palaeosol, when LREE were mobilised and fractionated in order to generate the observed patterns. The REE patterns and negative Ce anomalies observed by Mukhopadhyay *et al.* (2014) were likely generated then.

Conclusions

Combined ^{138}La-^{138}Ce, ^{147}Sm-^{143}Nd and ^{176}Lu-^{176}Hf isotope systematics demonstrate that the Ce anomalies in the Keonjhar Palaeosol cannot be taken as evidence for an elevated Archean oxygen partial pressure. ^{138}La-^{138}Ce and ^{176}Lu-^{176}Hf analyses indicate post-Mesoproterozoic REE mobilisation, including La-Ce fractionation, during alteration of the palaeosol. The observed REE patterns and Ce anomalies in the palaeosol suggest hydrothermal alteration and alteration processes at oxidising conditions. In addition, ^{147}Sm-^{143}Nd measurements argue for Proterozoic alteration and LREE mobilisation. Altogether, our data indicate multiple and complex element mobilisation processes during post-Archean alteration and hydrothermal overprint of the Keonjhar Palaeosol.

Acknowledgements

We thank A. Katzemich, Niklas Kallnik and Timo Lange for their support in the Lab and Mario Fischer-Gödde is thanked for the maintenance of the MC-ICP-MS. We thank the editor, Maud Boyet and an anonymous reviewer for constructive reviews that substantially improved the manuscript.

Editor: Gavin Foster

Additional Information

Supplementary Information accompanies this letter at https://www.geochemicalperspectivesletters.org/article2503.

Cite this letter as: Pfennig, M.L., Pakulla, J.J., Hasenstab-Dübeler, E., Wombacher, F., Jodder, J., Hofmann, A., Münker, C. (2025) Young oxygenation of the Archean Keonjhar Palaeosol, India, from ^{138}La-^{138}Ce chronometry. *Geochem. Persp. Let.* 33, 51–55. https://doi.org/10.7185/geochemlet.2503

References

Bandopadhyay, P.C., Eriksson, P.G., Roberts, R.J. (2010) A vertic paleosol at the Archean-Proterozoic contact from the Singhbhum-Orissa craton, eastern India. *Precambrian Research* 177, 277–290. https://doi.org/10.1016/j.precamres.2009.12.009

Banfield, J.F., Eggleton, R.A. (1989) Apatite Replacement and Rare Earth Mobilization, Fractionation, and Fixation During Weathering. *Clays and Clay Minerals* 37, 113–127. https://doi.org/10.1346/CCMN.1989.0370202

Barrat, J.-A., Bayon, G., Lalonde, S. (2023) Calculation of cerium and lanthanum anomalies in geological and environmental samples. *Chemical Geology* 615, 121202. https://doi.org/10.1016/j.chemgeo.2022.121202

Beukes, N.J., Mukhopadhyay, J., Gutzmer, J. (2008) Genesis of High-Grade Iron Ores of the Archean Iron Ore Group around Noamundi, India. *Economic Geology* 103, 365–386. https://doi.org/10.2113/gsecongeo.103.2.365

Bonnand, P., Lalonde, S.V., Boyet, M., Heubeck, C., Homann, M., Nonnotte, P., Foster, I., Konhauser, K.O., Köhler, I. (2020) Post-depositional REE mobility in a Paleoarchean banded iron formation revealed by La-Ce geochronology: A cautionary tale for signals of ancient oxygenation. *Earth and Planetary Science Letters* 547, 116452. https://doi.org/10.1016/j.epsl.2020.116452

Braun, J.-J., Pagel, M., Herbilln, A., Rosin, C. (1993) Mobilization and redistribution of REEs and thorium in a syenitic lateritic profile: A mass balance study. *Geochimica et Cosmochimica Acta* 57, 4419–4434. https://doi.org/10.1016/0016-7037(93)90492-F

Catling, D.C., Zahnle, K.J. (2020) The Archean atmosphere. *Science Advances* 6, eaax1420. https://doi.org/10.1126/sciadv.aax1420

Das, M., Monalisa, S.M., Paul, A.K., Mishra, R.K., Mohanty, J.K., Pradhan, A.A., Goswami, S. (2012) Geochemistry and Petrogenesis of Pyrophyllite Deposit of Madrangjodi, Keonjhar District, Orissa. *Journal of the Geological Society of India* 79, 460–466. https://doi.org/10.1007/s12594-012-0070-7

Dzombak, R.M., Sheldon, N.D. (2022) Terrestrial records of weathering indicate three billion years of dynamic equilibrium. *Gondwana Research* 109, 376–393. https://doi.org/10.1016/j.gr.2022.05.009

Farquhar, J., Peters, M., Johnston, D.T., Strauss, H., Masterson, A., Wiechert, U., Kaufman, A.J. (2007) Isotopic evidence for Mesoarchean anoxia and changing atmospheric sulphur chemistry. *Nature* 449, 706–709. https://doi.org/10.1038/nature06202

Haas, J.R., Shock, E.L., Sassani, D.C. (1995) Rare earth elements in hydrothermal systems: Estimates of standard partial molal thermodynamic properties of aqueous complexes of the rare earth elements at high pressures and temperatures. *Geochimica et Cosmochimica Acta* 59, 4329–4350. https://doi.org/10.1016/0016-7037(95)00314-P

Hayashi, T., Tanimizu, M., Tanaka, T. (2004) Origin of negative Ce anomalies in Barberton sedimentary rocks, deduced from La–Ce and Sm–Nd isotope systematics. *Precambrian Research* 135, 345–357. https://doi.org/10.1016/j.precamres.2004.09.004

Hofmann, A., Jodder, J., Xie, H., Bolhar, R., Whitehouse, M., Elburg, M. (2022) The Archean geological history of the Singhbhum Craton, India – a proposal for a consistent framework of craton evolution. *Earth-Science Reviews* 228, 103994. https://doi.org/10.1016/j.earscirev.2022.103994

Ludwig, K.R. (2001) User's Manual for Isoplot/Ex rev. 2.49. A Geochronological Toolkit for Microsoft Excel. *Berkeley Geochronology Center Special Publication* 1a, 1–55.

Lyons, T.W., Reinhard, C.T., Planavsky, N.J. (2014) The rise of oxygen in Earth's early ocean and atmosphere. *Nature* 506, 307–315. https://doi.org/10.1038/nature13068

Mukhopadhay, J., Crowley, Q.G., Ghosh, S., Gosh, G., Chakrabarti, K., Misra, B., Heron, K., Bose, S. (2014) Oxygenation of the Archean atmosphere: New paleosol constraints from eastern India. *Geology* 42, 923–926. https://doi.org/10.1130/G36091.1

Planavsky, N.J., Asael, D., Hofmann, A., Reinhard, C.T., Lalonde, S.V., Knudsen, A., Wang, X., Ossa Ossa, F., Pecoits, E., Smith, A.J.B., Beukes, N.J., Bekker, A., Johnson, T.M., Konhauser, K.O., Lyons, T.W., Rouxel, O.J. (2014) Evidence for oxygenic photosynthesis half a billion years before the Great Oxidation Event. *Nature Geoscience* 7, 283–286. https://doi.org/10.1038/ngeo2122

Pourmand, A., Dauphas, N., Ireland, T.J. (2012) A novel extraction chromatography and MC-ICP-MS technique for rapid analysis of REE, Sc and Y: Revising CI-chondrite and Post-Archean Australian Shale (PAAS) abundances. *Chemical Geology* 291, 38–54. https://doi.org/10.1016/j.chemgeo.2011.08.011

Rye, R., Holland, H.D. (1998) Paleosols and the evolution of atmospheric oxygen: A critical review. *American Journal of Science* 298, 621–672. https://doi.org/10.2475/ajs.298.8.621

Schnabel, C., Münker, C., Strub, E. (2017) La-Ce isotope measurements by multi-collector-ICPMS. *Journal of Analytical Atomic Spectrometry* 32, 2360–2370. https://doi.org/10.1039/C7JA00256D

Tait, J., Zimmermann, U., Miyazaki, T., Presnyakov, S., Chang, Q., Mukhopadhyay, J., Sergeev, S. (2011) Possible juvenile Palaeoarchaean TTG magmatism in eastern India and its constraints for the evolution of the Singhbhum craton. *Geological Magazine* 148, 340–347. https://doi.org/10.1017/S0016756810000920

Tanaka, T., Masuda, A. (1982) The La-Ce geochronometer: a new dating method. *Nature* 300, 515–518. https://doi.org/10.1038/300515a0

Tostevin, R. (2021) *Cerium Anomalies and Paleoredox*. Cambridge University Press, Cambridge. https://doi.org/10.1017/9781108847223

Yongliang, X., Yusheng, Z. (1991) The mobility of rare-earth elements during hydrothermal activity: A review. *Chinese Journal of Geochemistry* 10, 295–306. https://doi.org/10.1007/BF02841090